OPEN ACCESS

Original research

Ginseng polysaccharides alter the gut microbiota and kynurenine/tryptophan ratio, potentiating the antitumour effect of antiprogrammed cell death 1/programmed cell death ligand 1 (anti-PD-1/PD-L1) immunotherapy

Jumin Huang ,[1] Di Liu,[2] Yuwei Wang,[1] Liang Liu,[1] Jian Li,[3] Jing Yuan,[4] Zhihong Jiang,[1] Zebo Jiang,[1] WL Wendy Hsiao,[1] Haizhou Liu ,[2] Imran Khan,[1] Ying Xie,[1] Jianlin Wu,[1] Yajia Xie,[1] Yizhong Zhang,[1] Yu Fu,[1] Junyi Liao,[1] Wenjun Wang,[1] Huanling Lai,[1] Axi Shi,[1] Jun Cai,[1] Lianxiang Luo,[5] Runze Li,[1] Xiaojun Yao,[1] Xingxing Fan,[1] Qibiao Wu,[1] Zhongqiu Liu,[6] Peiyu Yan,[1] Jingguang Lu,[1] Mingrong Yang,[1] Lin Wang,[1] Yabing Cao,[7] Hong Wei,[3] Elaine Lai-Han Leung[1]

► Additional online supplemental material is published online only. To view, please visit the journal online (http://dx.doi.org/10.1136/gutjnl-2020-321031).

For numbered affiliations see end of article.

Correspondence to
Dr Elaine Lai-Han Leung, Macau University of Science and Technology State Key Laboratory of Quality Research in Chinese Medicines, Taipa, Macau 123, China; lhleung@must.edu.mo
Professor Hong Wei; weihong63528@163.com
Dr Yabing Cao; sumscaoyabing@hotmail.com

JH, DL and YW contributed equally.

Received 5 March 2020
Revised 5 April 2021
Accepted 4 May 2021
Published Online First 18 May 2021

To cite: Huang J, Liu D, Wang Y, *et al*. *Gut* 2022;**71**:734–745.

ABSTRACT

Objective Programmed death 1 and its ligand 1 (PD-1/PD-L1) immunotherapy is promising for late-stage lung cancer treatment, however, the response rate needs to be improved. Gut microbiota plays a crucial role in immunotherapy sensitisation and *Panax ginseng* has been shown to possess immunomodulatory potential. In this study, we aimed to investigate whether the combination treatment of ginseng polysaccharides (GPs) and αPD-1 monoclonal antibody (mAb) could sensitise the response by modulating gut microbiota.

Design Syngeneic mouse models were administered GPs and αPD-1 mAb, the sensitising antitumour effects of the combination therapy on gut microbiota were assessed by faecal microbiota transplantation (FMT) and 16S PacBio single-molecule real-time (SMRT) sequencing. To assess the immune-related metabolites, metabolomics analysis of the plasma samples was performed.

Results We found GPs increased the antitumour response to αPD-1 mAb by increasing the microbial metabolites valeric acid and decreasing L-kynurenine, as well as the ratio of Kyn/Trp, which contributed to the suppression of regulatory T cells and induction of T_{eff} cells after combination treatment. Besides, the microbial analysis indicated that the abundance of *Parabacteroides distasonis* and *Bacteroides vulgatus* was higher in responders to anti-PD-1 blockade than non-responders in the clinic. Furthermore, the combination therapy sensitised the response to PD-1 inhibitor in the mice receiving microbes by FMT from six non-responders by reshaping the gut microbiota from non-responders towards that of responders.

Conclusion Our results demonstrate that GPs combined with αPD-1 mAb may be a new strategy to sensitise non-small cell lung cancer patients to anti-PD-1 immunotherapy. The gut microbiota can be used as a novel biomarker to predict the response to anti-PD-1 immunotherapy.

Significance of this study

What is already known on this subject?

- The gut microbiota plays a crucial role in shaping the systemic immune system and has a major influence on the effectiveness of anticancer immunotherapy targeting the CTLA-4 and programmed death 1 and its ligand 1 (PD-1/PD-L1) pathways in both preclinical tumour models and patients with cancer.
- The response rate of non-small cell lung cancer (NSCLC) patients to anti-PD-1 immunotherapy is less than 25%, dietary supplements may influence the gut microbiome and the response to anti-PD-1 immunotherapy.
- Ginseng polysaccharides (GPs), one of the most abundant components of *Panax ginseng*, have an important influence on immunomodulation and antitumour effects.

INTRODUCTION

Lung cancer has the highest morbidity and mortality rate worldwide.[1] Approximately 80%–85% of all lung cancers are non-small cell lung cancers (NSCLCs). Inhibitors of programmed death 1 (PD-1) and its ligand PD-L1 are effective therapies for metastatic NSCLC lacking sensitising EGFR or ALK mutations.[2–6] However, even though these biomarkers were used as the gold standard, the response rate (<25%) is still unsatisfactory, even leading to hyperprogressive disease (HPD).[7 8] Hence, there remains a need for more effective first-line treatments for the majority of patients with advanced NSCLC and for predictive biomarkers to identify patients who may benefit from new therapies.[9] Extensive research has been carried out identifying new combinations of PD-1/PD- L1 pathway inhibitors with other treatments

Significance of this study

What are the new findings?

- GPs potentiated the antitumour effect of an αPD-1 monoclonal antibody (mAb) in Lewis lung cancer-bearing mice.
- Combination therapy with GPs and an αPD-1 mAb increased the activated $CD8^+$ T cell population and reduced the $Foxp3^+$ regulatory T cell population in the periphery, consistent with a decrease in the kynurenine/tryptophan ratio.
- NSCLC responders and non-responders to pembrolizumab exhibited distinct gut microbiota diversity as detected by 16S PacBio SMRT sequencing, and two differentially abundant species, *Parabacteroides distasonis* and *Bacteroides vulgatus* were found.
- Combination therapy with GPs and αPD-1 mAb reshaped the composition of the gut microbiota from non-responders towards that of the responders, which reinstated the response to the αPD-1 mAb in mice transplanted with PD-1 non-responder faecal samples.

How might it impact on clinical practice in the foreseeable future?

- Gut microbiota status, such as alpha diversity, can be used as a biomarker to predict the response to anti-PD-1 immunotherapy in NSCLC patients.
- GPs represent a novel class of prebiotics to enhance the response to anti-PD-1 immunotherapy in NSCLC patients.
- *P. distasonis* and *B. vulgatus* can be used as adjuvants for anti-PD-1 immunotherapy.

or drugs with immunomodulatory effects which may enhance antitumour response.[10 11] Recently, gut microbiota has fuelled great enthusiasm in cancer immunotherapy. Such as *Bacteroides fragilis*, *Bacteroides thetaiotaomicron*, *Bifidobacterium*, *Akkermansia muciniphila* and *Faecalibacterium* spp. have been shown to have favourable responses to cancer immunotherapy in both preclinical tumour models and patients with cancer.[12–15] Strategies to modulate gut microbiota have thus been proposed to treat patients with cancer and act as novel response prediction biomarkers.

Panax ginseng has been widely used in Asia for thousands of years, not only as a medicine but also as a dietary supplement. The long-term administration of ginseng extracts has been shown to modulate the rat gut microbiota by increasing the abundance of *Bifidobacterium*, *Allobaculum*, *Lactobacillus*, *Clostridium* and *Parasutterella*.[16] Quan *et al* reported that the whole extract of ginseng specifically increases the abundance of *Enterococcus faecalis*, which contributes to the antiobesity effect of its long-chain fatty acid metabolite myristoleic acid.[17] Ginseng contains many active components, including ginsenosides, essential oils, peptidoglycans, polysaccharides, nitrogen-containing compounds, fatty acids and phenolic compounds.[18] Among these components, ginseng polysaccharides (GPs) have been demonstrated to be responsible for the immunomodulatory functions, such as the activation of macrophages, T cells and natural killer cells. Moreover, GPs improve intestinal metabolism and modulate the gut microbiota and particularly enhance the growth of *Lactobacillus* spp. and *Bacteroides* spp., two major species of bacteria that metabolise ginsenosides.[19 20] Nevertheless, the therapeutic potential of GPs has not been well explored in cancer immunotherapy. The main goal of our present study was to define the synergistic antitumour effect of GPs and investigate whether the potential effect is related to gut microbiota modulation and its associated treatment mechanisms.

METHODS

Mouse experiments

The 8–12 weeks old C57BL/6J mice and humanised PD-1 knock-in (HuPD-1) mice were reared in independently vented cages at the animal facility of the State Key Laboratory of Quality Research in Chinese Medicine, Macau University of Science and Technology.

Approximately 5×10^5 Lewis lung cancer (LLC) cells and 5×10^4 B16-F10 cells were subcutaneously inoculated into the right flanks of mice. A total of 24 mice from different litters were equally divided into four groups: Vehicle (treated with PBS), αPD-1 monoclonal antibody (mAb) (250 µg/mouse, clone: RMP1-14, Bio X Cell), GPs (200 mg/kg) and GPs plus αPD-1 mAb group. Daily oral treatment with GPs was administrated after tumour inoculation and injection of αPD-1 mAb 5 times at 3-day intervals on day 9 when tumour volumes were approximately 50 mm^3. Tumour volumes and body weights were measured every 3 days.

Antibodies and flow cytometry

At the endpoint of the experiment, the blood, spleen and tumours were harvested for flow cytometry analysis. Lamina propria mononuclear cells (LPMCs) were isolated using a LP dissociation kit (Miltenyi Biotec, Germany) according to the manufacturer's instructions. Initially, the intraepithelial lymphocytes (IELs) were disrupted from the mucosa by shaking the tissue in a predigestion solution. Then, the LP tissue was further treated enzymatically and mechanically dissociated into a single-cell suspension containing LPMCs by using a gentle MACS dissociator.

For FACS analysis, single-cell suspensions were stained with the following antibodies: PerCP anti-mouse CD45, APC anti-mouse CD3, FITC anti-mouse CD4, and PE/Cy7 anti-mouse CD8 (Biolegend, clone 30-F11; clone 17A2, clone RM4-5, and clone 53–6.7, respectively, USA). For intracellular staining, cells were stimulated for 4–6 hour at 37°C with PMA (50 ng/mL), ionomycin (1 µg/mL) and BD Golgi STOP^T. After being fixed and permeabilised, the cells were stained with APC/Cy7 anti-mouse interferon (IFN)-γ, PE/Dazzle 594 tumour necrosis factor (TNF)-α, PE antimouse granzyme B (GZMB), PE antimouse FoxP3, PerCP/Cy5.5 antimouse ROR-γt and PE anti-mouse interleukin-17A (Biolegend, clone XMG1.2, clone 506346, clone: 259D, clone MF-14, clone Q31-378, and clone TC11-18H10.1, respectively, USA). Flow cytometry analysis was performed using a FACSArial III flow cytometer (BD, USA). Data were analysed using FlowJo software (V.10.4, FlowJo, USA).

Metabolomic profiling of short-chain fatty acids and tryptophan in the plasma

The mouse blood samples were centrifuged at 3000 rpm for 15 min, and the supernatants were collected. The samples were then derivatised and analysed using ultraperformance liquid chromatography-mass spectrometry (UPLC-MS). Short-chain fatty acids (SCFAs), L-kynurenine, and L-tryptophan in the plasma were determined by following a modified protocol as previously described.[21 22]

Histopathological scoring and immunohistochemical staining

Tumour tissues and colons were dissected and partially embedded in 4% PFA for 48 hours. Paraffin-embedded tissue sections

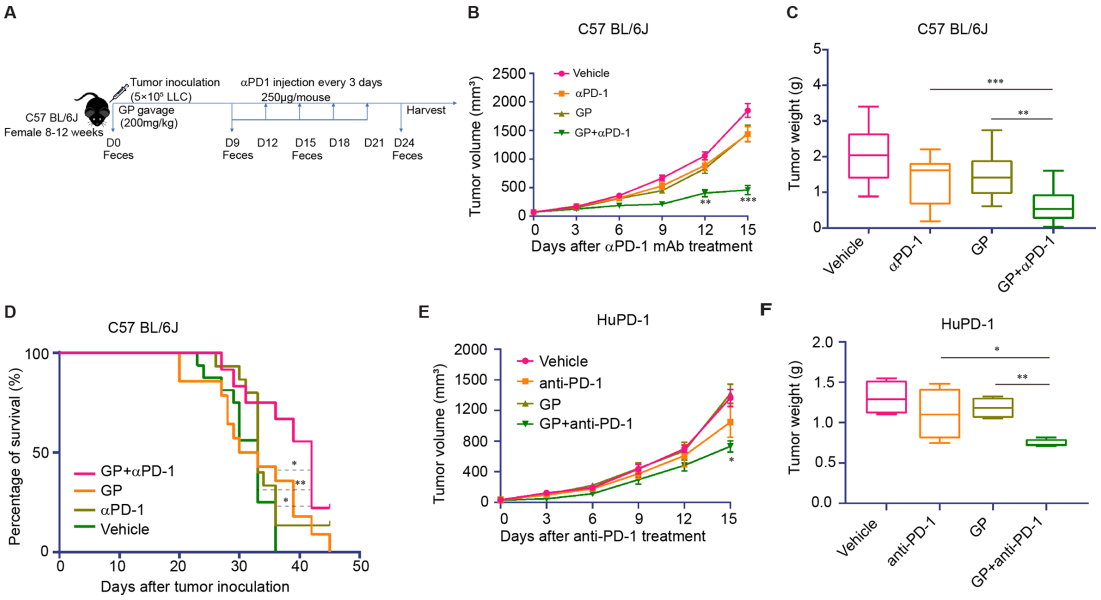

Figure 1 GPs potentiate the antitumour effect of the αPD-1 mAb in conventional and humanised PD-1 knock-in (HuPD-1) LLC-bearing mice. (A) Schematic diagram of the GPs plus αPD-1 mAb treatment in LLC-bearing mice. (B) Tumour growth curves were shown in each group. Conventional C57 BL/6J mice were received GPs on day 0 and intraperitoneally injected with αPD-1 mAb on day nine after tumour inoculation. (C) Tumour weight of the conventional LLC-bearing mice. (D) Survival curve of the conventional LLC-bearing mice. (E) Tumour growth curves were shown in each group in huPD-1 knock-in LLC-bearing mouse model. (F) Tumour weight of the HuPD-1 knock-in tumour-bearing mice. Data were representative of one or three independent experiments with n=5–10 per group. Error bars represent the mean±SEM. Tumour growth curves were assessed by two-way ANOVA with Sidak correction. Tumour weight was assessed by one-way ANOVA. Log-rank (Mantel-Cox) tests were performed for survival data. *P<0.05, **p<0.01, ***p<0.001. ANOVA, analysis of variance; GPs, ginseng polysaccharides; LLC, Lewis lung cancer; mAb, monoclonal antibody; PD-1, programmed death 1.

(5 μm) were stained with H&E for morphological examination. Immunohistochemical staining (IHC) was performed to evaluate the expression of CD4, CD8, IFN-γ, TNF-α, GZMB and IDO using immunohistochemistry kits (K8002; Dako, Glostrup, Denmark) according to the manufacturer's protocol. Slides were scanned and observed under a Leica optical microscope (Leica Biosystems Imaging, USA).

Fecal microbiota transfer experiment

Faecal pellets from six NR were homogenised in 10 mL of sterile saline. Then, 200 μL of the suspension was transferred by oral gavage into each germ-free (GF) mouse (6–8 weeks old). Besides, another 100 μL was applied to the fur of each animal. GF mice were gavaged with faecal samples 3 times for 2 weeks. GF mice were maintained in a gnotobiotic isolator with irradiated food and autoclaved water at the Third Army Medical University (Chongqing, China) and the First Affiliated Hospital, Sun Yat-Sen University. Two weeks after faecal microbiota transplantation (FMT), tumour cells were inoculated, and the mice were treated with GPs and/or αPD-1 mAb as mentioned above.

RNA-sequencing of IELs

IELs were isolated as described previously with slight modification.[23] Total RNA was extracted as instruction of RNeasy Plus Micro Kit (Qiagen, Germany). The detailed sequencing and differential expression analysis methods are described in online supplemental methods.

Fecal DNA extraction and 16S rRNA sequencing

Total genomic DNA of patients and mouse faecal samples were extracted using QIAamp PowerFecal DNA kits (Qiagen, Hilden, Germany) or Shoreline Complete StrainID Kit (Shoreline Biome, USA), respectively, according to the manufacturer's instructions. The DNA concentration and purity were monitored on 1% agarose gels. Amplicon libraries were created using PacBio SMRTbell Express Template Prep Kit V.3.0 (PacBio) and sequenced on a PacBio Sequel System at Macau University of Science and Technology according to the manufacturer's recommendation. SBanalyzer V.3.0 (Shoreline Biome) was used to assign taxonomic identification to all reads mapped to Athena database.[24] QIIME 2 was used for further analysis.

Statistical analysis

All data are expressed as the mean±SEM The differences between groups were analysed by two-way analysis of variance (ANOVA) or one-way ANOVA. The critical p value was set to 0.05 for significant differences. Statistical analysis was performed by GraphPad Prism V.8.0.2 (San Diego, California, USA). A value of $p<0.05$ was considered statistically significant.

RESULTS

Combination therapy sensitises the antitumour effect of αPD-1 mAb in tumour-bearing mouse models

To investigate whether GPs can enhance the antitumour effect of αPD-1 mAb, we first evaluated tumour growth and progression in C57 BL/6J mice-bearing LLC. GPs oral gavage and αPD-1 mAb injection began to be administered to mice on days 0 and 9 post-tumour inoculation, respectively (figure 1A). The antitumour effect was initially evaluated by tumour volume and tumour weight (figure 1B,C). After combination treatment, the conventional LLC-bearing mice exhibited an increased response to αPD-1 mAb and reduced tumour progression (online supplemental figure 1A). On day 24, the combination treatment group exhibited 75.2% and 65.1% tumour growth suppression

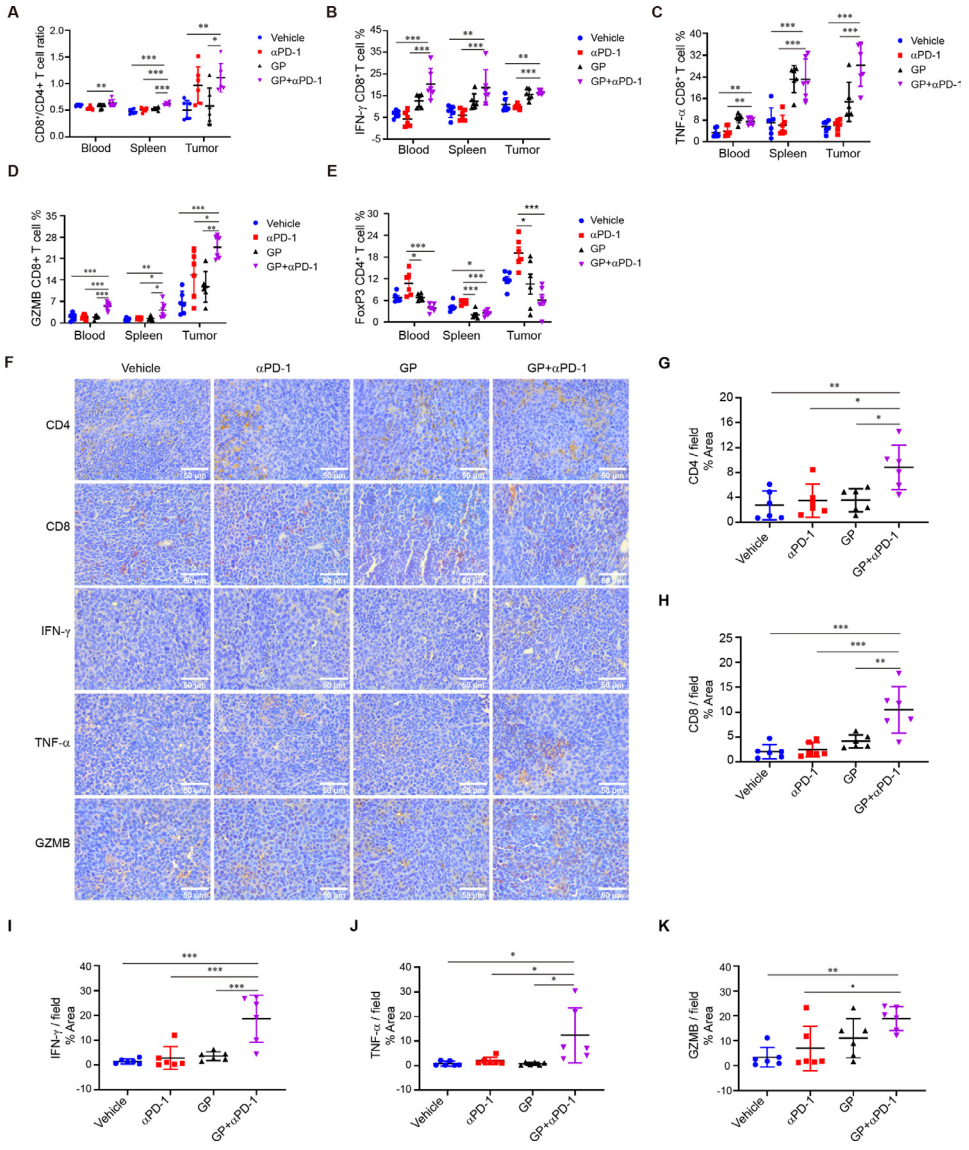

Figure 2 The cytotoxic CD8$^+$ T cell population increases, whereas the Treg cell population decreases after treatment with the combination therapy. In conventional LLC-bearing mice, 24 days after tumour inoculation, the mice were treated with the αPD-1 mAb, GPs, or a combination of GPs and the αPD-1 mAb. Immune cells in the blood, spleen and tumour were analysed. (A–E) CD8$^+$/CD4$^+$ T cell ratio, expression of IFN-γ, TNF-α, granzyme B (GZMB) among CD8 +T cells and FOXP3 CD4+ T cells in the blood, spleen and tumour tissues. (F) Representative IHC profiles of CD4, CD8, IFN-γ, TNF-α and GZMB in tumour tissues at ×400 magnification. Scale bar=50 µm. (G–K) Quantitative analysis of positive area per field by image J software (NIH) with ImmunoRatio Plugin. Data presented as means of 15 fields and expressed as mean±SD (n=6). All experiments were repeated two or three times. Each symbol represents an individual animal. Data represent the mean±SD and were analysed by one-way ANOVA. *P<0.05, **p<0.01, ***p<0.001. ANOVA, analysis of variance; GPs, ginseng polysaccharides; IFN-γ, interferon-γ; IHC, immunohistochemistry; LLC, Lewis lung cancer; mAb, monoclonal antibody; TNF-α, tumour necrosis factor-α; Treg, regulatory T cells.

compared with the Vehicle and αPD-1mAb treatment alone group, respectively. Correspondingly, the survival of mice was significantly prolonged (figure 1D). These results indicate that combination treatment improves the antitumour effect of αPD-1 mAb in LLC-bearing mice. We also observed this potentiated antitumour effect in HuPD-1 mice with LLC cells (figure 1E,F) and B16-F10 tumour-bearing mice (online supplemental figure 1B,C).

In vivo antitumour effect of the combination treatment is associated with increased immunity

To determine the effects of the combination therapy on the immune system, we analysed the immunological changes in the peripheral blood, spleen and tumour tissues using flow cytometry. We observed that CD8$^+$/CD4$^+$ ratio in the combinational group increased in both peripheral (blood and spleen tissues) and tumour tissues when compared with αPD-1 mAb alone group (figure 2A). The production of functional cytokines, IFN-γ, TNF-α andGZMB among CD8$^+$ T cells also increased both in peripheral and tumour tissues (figure 2B–D, (online supplemental figure 2), indicating the beneficial effect of the drug combination. Meanwhile, we also observed the downregulation of FoxP3$^+$ regulatory T (Treg) cells in peripheral and tumour tissues (figure 2E). And the IHC profiles got consistent results in tumour tissues (figure 2F–K). These results indicated that combination treatment may take effect by activating CD8$^+$ T cells and suppressing the function of Tregs.

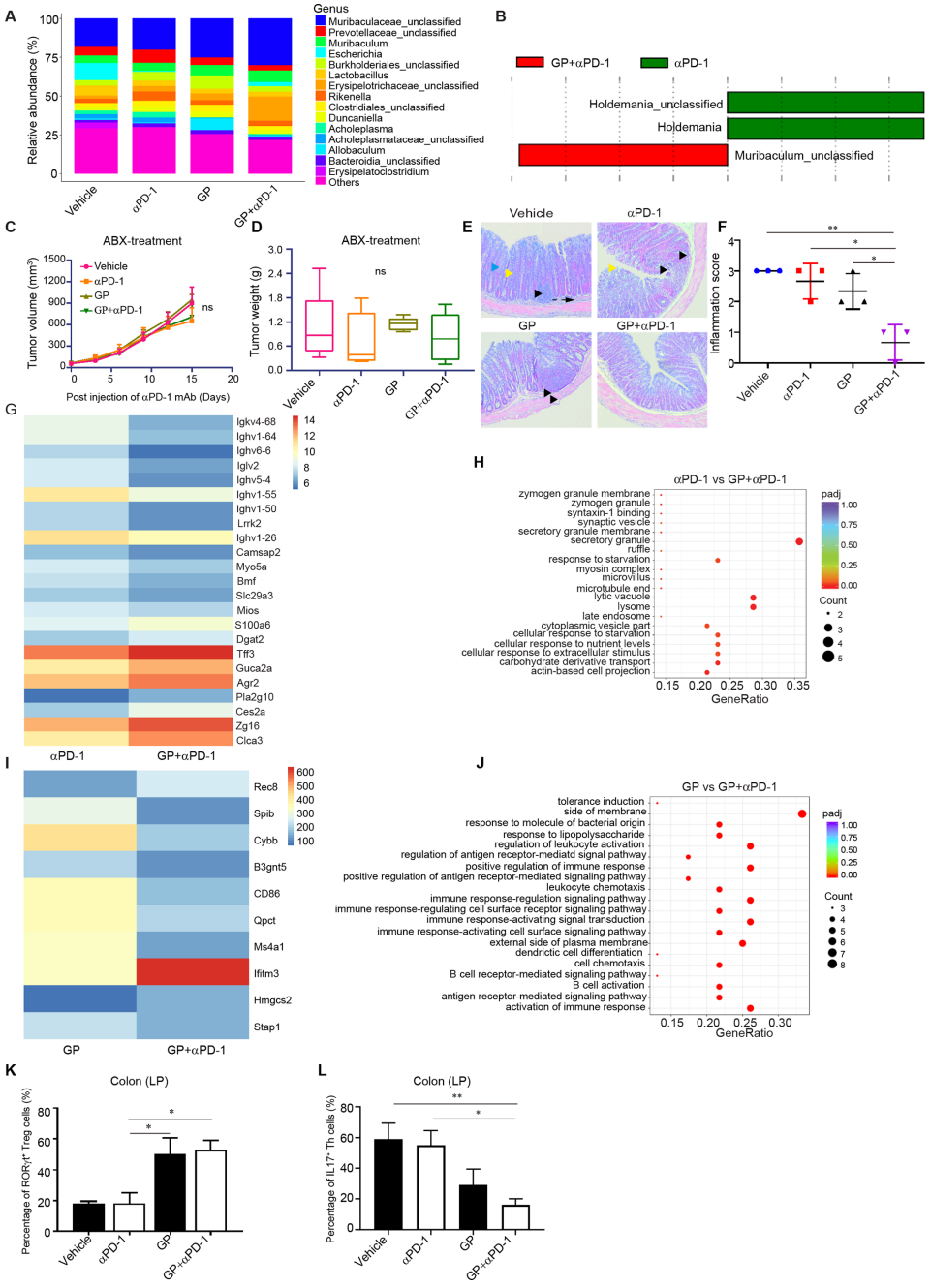

Figure 3 Combination treatment maintains gut homeostasis by modulating gut microbiota and enhancing gut immunity. (A) Relative abundance of top 15 genera in different treatment groups. (B) LEfSe analysis for differential abundant taxa detected between αPD-1 mAb and combination group. Threshold parameters were set as p=0.05 for the Mann-Whitney U test and multiclass analysis=all against all. LDA score >2.0. (C) Tumour growth curve from four groups treated with vehicle, αPD-1 mAb, GP and combination GP and αPD-1 mAb, respectively, on day 9 after tumour inoculation and antibiotics (ABX) were administrated 2 weeks before tumour inoculation and continued until the end of the experiment. (D) Tumour weight of ABX-treated tumour-bearing mice. Data are representative with n=6 per group. (E, F) Histomorphology of the colon in LLC-bearing mice and inflammation score was evaluated. Score 0: normal colon mucosa with intact epithelium; score 1: scattered inflammatory cell infiltrates in the mucosa; score 2: diffuse mucosal infiltrates without submucosal spreading and intact epithelial layer; score 3: moderate infiltration of inflammatory cells into mucosa and submucosa with epithelial hyperplasia and goblet cell loss; score 4: marked inflammatory cell infiltrates in mucosa and submucosa accompanied by crypt abscesses and loss of goblet cells and crypts; score 5: marked inflammatory cell infiltrates within the mucosa spreading to the submucosa going along with crypt loss and haemorrhage. Original magnification ×100; scale bars 100 µm; black arrowhead-inflammatory cell infiltrates within mucosa (solid) and submucosa (dotted); yellow arrowhead-goblet cell loss. (G, H) Heatmaps showing differential genes and gene ontology (GO) functional analysis in IELs of small intestine between αPD-1 versus combination group and GP versus combination group. (I, J) Heatmaps showing differential genes and GO functional analysis in IELs of small intestine between GP versus combination group and GP versus combination group. Top 20 significantly enriched go terms in cellular compares, molecular function and biological process are presented. GO terms with padj <0.05 are significant enrichment. (K, L) Levels of RORγt$^+$ Treg and Th17 cells in colon laminar propria. data represent mean±SD and analysed by Mann-Whitney U test or Kruskal-Wallis test. *P<0.05, **p<0.01. GPs, ginseng polysaccharides; IELs, intraepithelial lymphocytes; LLC, Lewis lung cancer; mAb, monoclonal antibody; Treg, regulatory T cells.

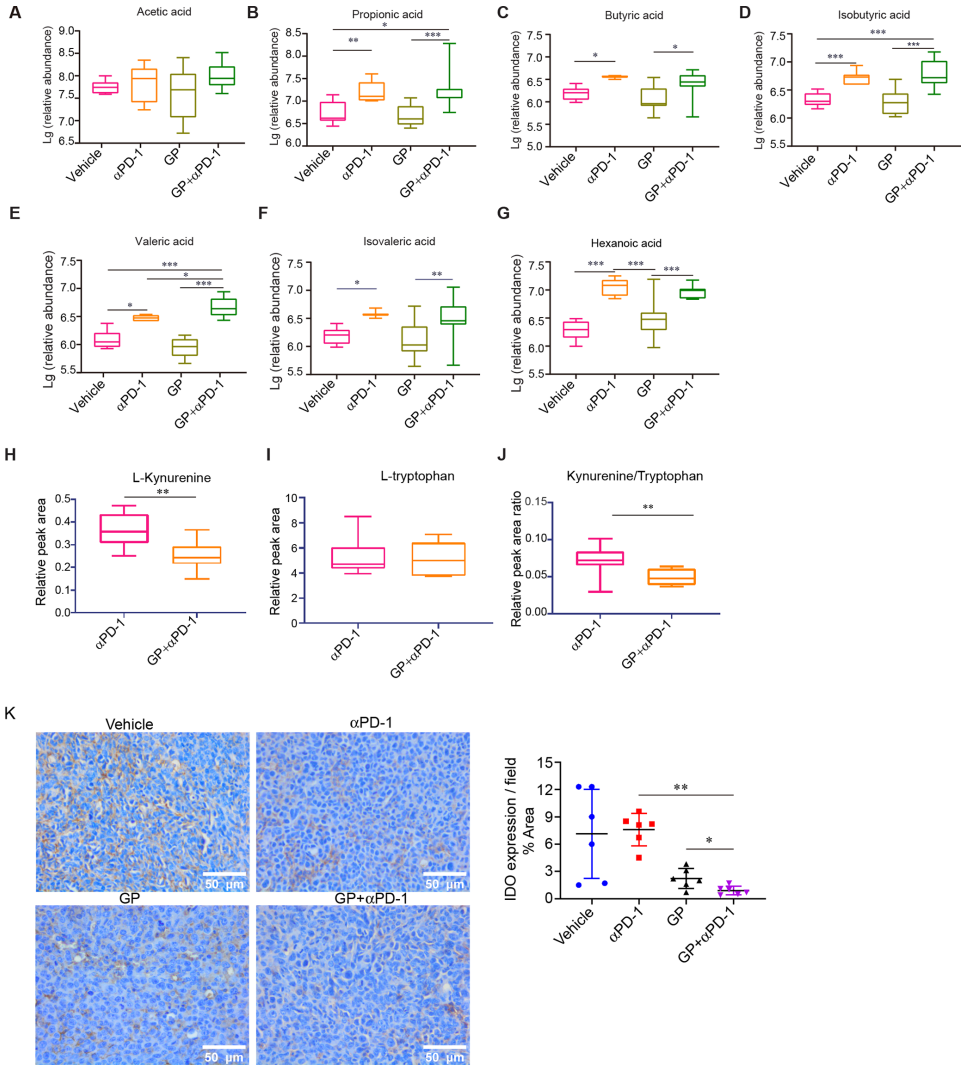

Figure 4 SCFAs abundance increases and IDO activity decreases after combination treatment. SCFAs, fatty acids and amino acids in the plasma were detected using UPLC-MS. (A–G) Relative abundance of SCFAs, including acetic acid, propionic acid, butyric acid, isobutyric acid, valeric acid, isovaleric acid and hexanoic acid, in the LLC-bearing model mice. (H–J) Relative peak areas of L-kynurenine, L-tryptophan and kynurenine/tryptophan. (K) Representative IHC profiles of IDO in LLC tumour tissues at ×400 magnification. scale bar=50 μm. (L) Quantitative analysis of positive area per field by image J software (NIH) with ImmunoRatio Plugin. Data presented as means of 15 fields and expressed as mean±SD (n=6). Data were analysed by one-way ANOVA or Student's t-test. *P<0.05, **p<0.01, ***p<0.001. ANOVA, analysis of variance; IHC, immunohistochemistry; UPLC-MS, ultra-performance liquid chromatography and mass spectrometry; LLC, Lewis lung cancer; SCFAs, short-chain fatty acids;

Regulatory T cells (Tregs) are major players in the immunosuppressive tumour microenvironment, which is frequently associated with poor prognosis and survival.[25] Clinical studies have identified a group of patients who may experience increased rapid cancer HPD risk after anti-PD-1 treatment due to the increased proliferation of FoxP3$^+$ Treg cells, hindering the application of immunotherapy.[26 27] In our study, GPs combined with αPD-1 mAb reduced the proportion of FoxP3$^+$ Tregs both in the periphery and tumour, which may contribute to preventing HPD. Altogether, these data indicate the enhanced antitumour immunity effect of combination treatment.

Combination treatment prevents gut microbiota dysbiosis

To investigate whether gut microbiota is altered by oral GPs administration, we performed 16S PicBio SMRT sequencing on faecal samples from all treatment groups. After combination treatment, the microbial composition was changed and the abundance of *Muribaculum* was significantly increased compared with αPD-1 mAb alone group (figure 3A,B). We also observed the increase of *Muribaculaceae* when compared GP and Vehicle group (online supplemental figure 3), which indicated that GPs may have the potential to enrich the abundance of *Muribaculaceae*. To further elucidate the causal relationship between the gut microbiota and the antitumour effects, we evaluated the tumour growth in LLC-bearing mice treated with antibiotics and found antibiotic treatment compromised the antitumour efficacy (figure 3C,D). In terms of the maintenance of intestinal immunity, histopathological evaluation of the colon revealed that the combination treatment could reduce the infiltration of inflammatory cells in the colon (figure 3E,F).

IELs play a vital role in maintaining barrier function and decreasing susceptibility to infection and immunopathology. To investigate whether the combination treatment impacts IELs, we adopted RNA-sequencing to examine the transcriptome changes of IELs in the small intestine. Compared with that in the αPD-1 mAb alone group, the expression of intraepithelial protection

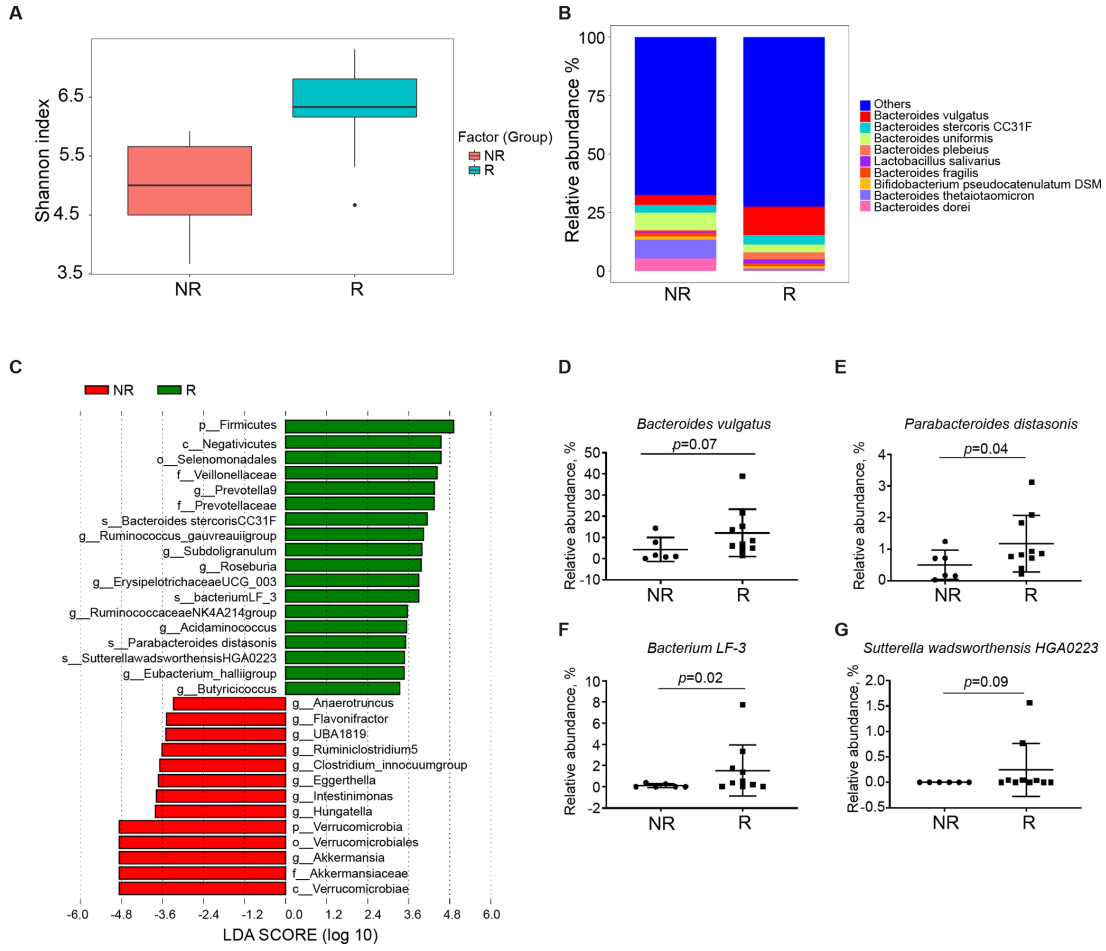

Figure 5 Comparison of the gut microbiota diversity between responders (Rs) and non-responders (NRs) sequenced by 16S PacBio SMRT sequencing. (A) Shannon index in the Rs (n=10) and n=6) groups. (B) Histogram of relative abundance of the top 10 at species level with respect to each group. (C) LEfSe analysis for differential abundant taxa detected between Rs and NRs before treatment with pembrolizumab. Threshold parameters were set as p=0.05 for the Mann-Whitney test and multiclass analysis=all against all. Linear discriminant analysis (LDA) score >2.0. (D–G) Differential bacteria between Rs and NRs. Data represent mean±SD and analysed by Mann-Whitney U test.

genes (CLCA3, Zg16, Pla2g10, Agr2, Guca2a and Tff3),[28–30] metabolism-related genes (Dgat2 and Ces2a)[31 32] and S100A6 was significantly upregulated in the combination treatment group. Conversely, the expression of immunoglobulin variable region heavy chain genes (Ighv1-64, Ighv6-6, Ighv5-4, Ighv1-55, Ighv1-50 and Ighv1-26), immunoglobulin variable region light chain genes (Iglv2), immunoglobulin kappa variable genes (Igkv4-68), Lrrk2, Camsap2, Myo5a, Bmf, Slc29a3, and Mios was downregulated in the IELs from mice treated with combination therapy (figure 3G). Gene ontology (GO) analysis revealed that these differentially expressed genes were mainly associated with the lysosome, secretory granule and energy metabolism, which can protect the integrity of the gut barrier (figure 3H). When compared with GP alone group, we observed that the immune response-rated genes were upregulated in the combination group (figure 3I,J).

RORγt$^+$ Treg cells can be induced in the gut in response to microbial stimuli.[33] The balance between RORγt$^+$ Treg cells and Th17 cells can help to maintain gut homeostasis. To observe the protective effect on the intestinal tract, we examined the proportions of RORγt$^+$ Treg cells and Th17 cells in the LP of the colon. As expected, increased proportions of RORγt$^+$ Treg cells and reduced proportions of Th17 cells were found in the combination treatment group (figure 3K,L).

Combination treatment increases SCFA abundance and dysregulates indoleamine 2,3-dioxygenase (IDO) activity

RORγt$^+$ Tregs are induced by microbiota through SCFAs.[33] SCFAs are crucial metabolites that can serve as an energy source and prevent intestinal epithelial cells and lymphocytes from undergoing autophagy due to nutrient starvation.[34] SCFAs in the host are not limited to the gut; they can also disseminate into the blood and thus communicate with multiple cells in target tissues in a G-protein-coupled receptors (GPCR)-dependent manner or by suppressing histone deacetylases (HDAC) epigenetic activity.[35] Thus, SCFAs may mediate the contribution of the microbiota to cancer immunity. To investigate the effect of SCFAs, we detected SCFAs (acetic acid, propionic acid, butyric acid, isobutyric acid, valeric acid, isovaleric acid and hexanoic acid) production in the plasma of animals using ultra-performanceliquid chromatography-mass spectrometry (UPLC/MS). Interestingly, we found that the abundance of all the SCFAs increased after treatment with αPD-1 mAb except for acetic acid; notably, the abundance of valeric acid was significantly increased in the combination treatment group compared with αPD-1 mAb alone group (figure 4A–G).

Other than SCFAs, we also measured 52 amino acids and fatty acid metabolites changes (online supplemental figure 4A).

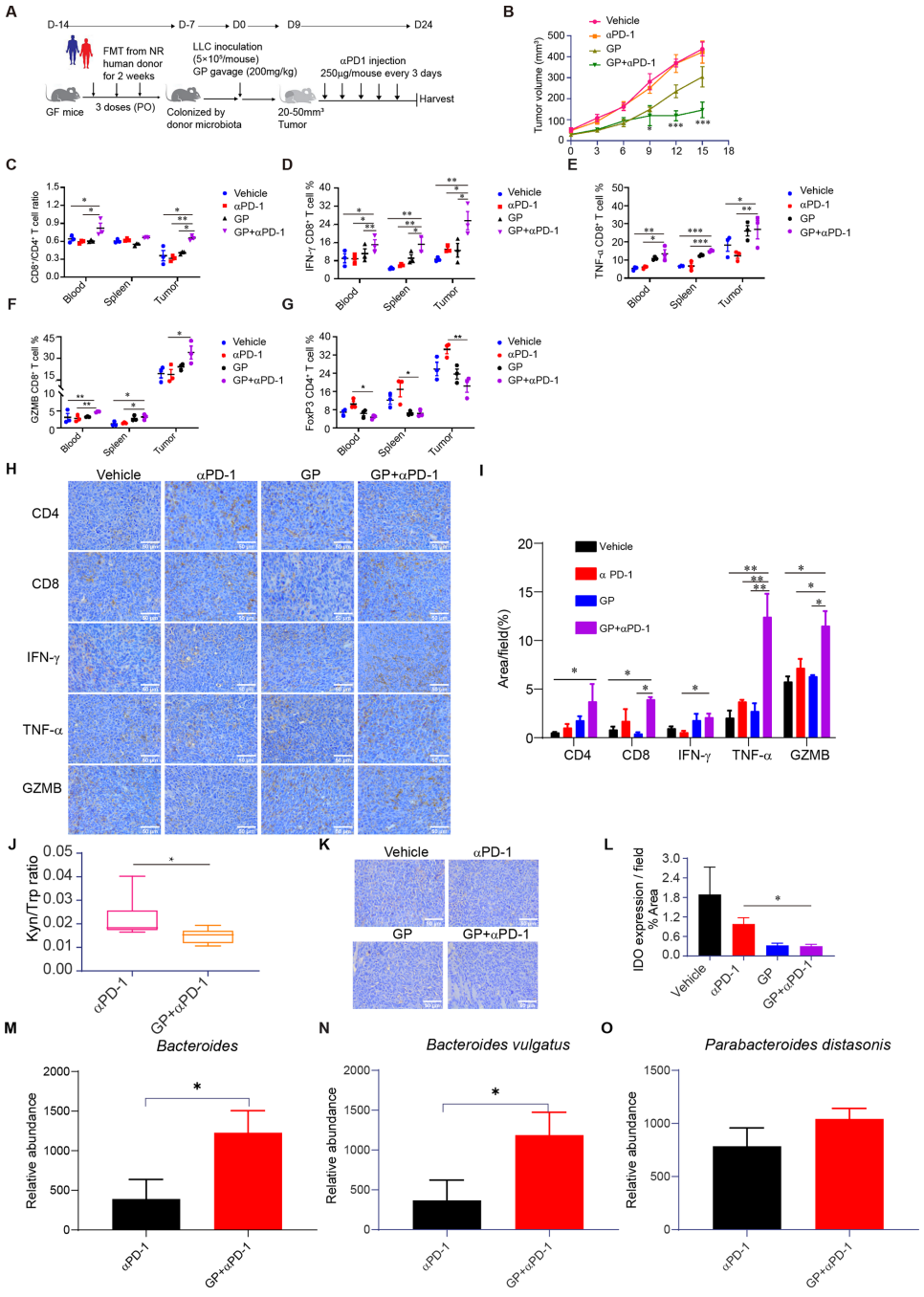

Figure 6 GPs reinstate the response to αPD-1 mAb in LLC tumour-bearing mice transplanted microbiota from non-responders. (A) Schematic diagram of FMT experiment. (B) Tumour growth curves in each group. error bars represent the mean±SEM Tumour growth curves were assessed by two-way ANOVA with Sidak correction. (C–G) $CD8^+/CD4^+$ T cell ratio, expression of IFN-γ, TNF-α, granzyme B (GZMB) among CD8 +T cells and $Foxp3^+$ $CD4^+$ T cells in the blood, spleen and tumour tissues. (H) Representative IHC profiles of CD4, CD8, IFN-γ, TNF-α and GZMB in tumour tissues at ×400 magnification. scale bar=50 μm. (I) Quantitative analysis of positive area per field by image J software (NIH). Data presented as mean of 15 fields and expressed as mean±SD (n=3) and were analysed by one-way ANOVA. Each symbol represents an individual animal. *P<0.05, **p<0.01, ***p<0.001. (J) Kynurenine/tryptophan ratio in mice plasma which transferred microbiota from NRs. (K) Representative IHC profiles of IDO in tumour tissues from microbiota colonised mice. (L) Quantitative analysis of positive area per field of IDO expression by image J software (NIH). (M) Relative abundance of *Bacterorides* in αPD-1 mAb and combination group. (N) Relative abundance of *Bacteroides vulgatus* in αPD-1 mAb and combination group. (O) Relative abundance of *Parabacteroides distasonis* in αPD-1 mAb and combination group. ANOVA, analysis of variance; GPs, ginseng polysaccharides; IFN-γ, interferon-γ; mAb, monoclonal antibody; IHC, immunohistochemistry; NR, non-responder; TNF-α, tumour necrosis factor-α.

We observed tryptophan metabolism contributes most among these metabolites with a marked decrease of L-kynurenine and the ratio of Kyn/Trp (expressed as IDO activity) but not L-tryptophan in the combination treatment group compared with the αPD-1 mAb alone group (online supplemental file 4A–D, Figure 4H–J). The results indicated that combination treatment may be associated with IDO activity. To further investigate the IDO activity in tumour tissues, we performed IHC staining and found the expression of IDO in the combination group was downregulated (figure 4K). To determine the effect

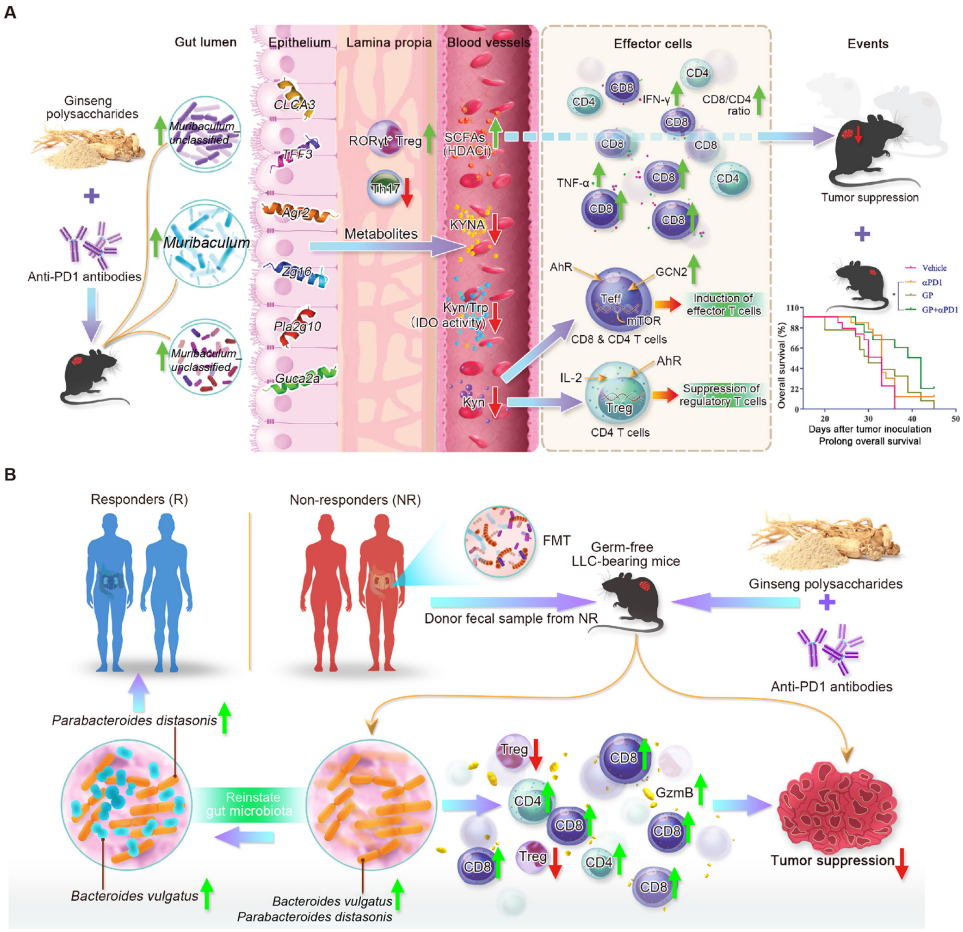

Figure 7 GPs combined with αPD-1 mAb improve the response rate by reinstating the gut microbiota. (A) GPs potentiated the antitumour effect with αPD-1 mAb via enhancing CD8 T cells function, increasing the production of IFN-γ and TNF-α and reducing the suppression effect of Treg in circulating system, which might be addressed by reshaping gut microbiota and thus influencing tryptophan metabolism and SCFAs. Combination treatment enriched the abundance of *Muribaculum* when administrated into LLC-bearing mice. Combination treatment upregulated the expression of epithelium protecting genes, like CLCA3, TFF3, AGR2, Zg16, Pla2g10 and Guca2a. The metabolites SFCAs and kynurenine trafficked into circulating system and enhanced the immune function thus suppressing tumour growth and prolonging survival. (B) Combination therapy reinstated gut microbiota which helps to revert gut microbiota from non-responders to responders, thus potentiating the response to αPD-1 mAb. 16S SMRT sequencing found *Parabacteroides distasonis* and *Bacteroides vulgatus* were higher in abundance in responders to pembrolizumab. When transplanted the gut microbiota from non-responders to germ-free mice by faecal microbiota transplantation (FMT) and then inoculated LLC tumour cells after colonisation, combination therapy was administrated to the mice. A rich abundance of *B. vulgatus and P. distasonis* were found in combination group by 16S PacBio SMRT sequencing compared with αPD-1 mAb and vehicle group. Meanwhile, combination therapy significantly suppressed tumour growth by enhancing the function of $CD8^+$ T cells, increasing the production of IFN-γ, TNF-α, and granzyme B and decreasing Treg cells. GPs, ginseng polysaccharides; IFN-γ, interferon-γ; LLC, Lewis lung cancer; mAb, monoclonal antibody; IHC, immunohistochemistry; NRs, non-responder; SFCAs, short-chain fatty acids; TNF-α, tumour necrosis factor-α.

of GPs on tryptophan metabolism in gut microbes, we meta-fermented human faecal samples with GPs by an in vitro batch fermentation system. Interestingly, we found that GPs markedly increased the production of L-tryptophan and reduced the production of L-kynurenine, as well as the kynurenine/tryptophan ratio both under aerobic and anaerobic fermentation conditions (online supplemental table 1), suggesting that GPs could influence tryptophan metabolism through gut microbes.

Distinct gut microbiota composition is present in pembrolizumab-treated NSCLC responders and non-responders

Sixteen Chinese patients with NSCLC were enrolled and treated with anti-PD-1 blockade. Ten of these patients were classified as responders (Rs), and six as non-NRs (NRs) assessed by a physician at Kiang Wu Hospital in Macau. The clinical-pathological features of these patients are listed in online supplemental table 2). All patients were followed up over 30 months, and their response status was monitored with CT scans (online supplemental figure 5A–C).

To investigate whether the composition of the gut microbiome was associated with anti-PD-1 immunotherapy, baseline faecal samples were collected and subjected to 16S PacBio SMRT sequencing. The alpha diversity of the gut microbiome suggested that the richness and evenness of the Rs were higher than those of the NRs (figure 5A). At the species level, we observed that the relative abundance of *Bacteroides vulgatus* accounts for the top of the list in Rs, as well as an overrepresentation of three gut microbes: *Parabacteroides distasonis* (p=0.04), *bacterium LF-3* (p=0.02) and *Sutterella wadsworthensis HGA0223* (p=0.09; figure 5B–G, (online supplemental file 5D–G). Interestingly, the

abundance of these bacteria was increased in patients who had better response and survival rates.

GPs reinstate the response to αPD-1 mAb treatment in LLC-bearing mice transplanted with feces from non-Rs

In our initial study, we found that GPs potentiated the antitumour effect of αPD-1 mAb in LLC-bearing mice. Whether GPs could reverse the response to αPD-1 mAb treatment in humans remains unknown; therefore, we designed an FMT experiment to investigate it. Faecal microbiota from the six NRs was transferred into GF mice. When colonised, the mice were inoculated with LLC tumour cells. Then, mice were treated with the same mouse protocol as previously used (figure 6A). As expected, similarly to the NRs, we found that mice were resistant to αPD-1 mAb treatment. Interestingly, when mice were treated with GPs plus αPD-1 mAb, the response was reinstated. The combination treatment significantly delayed tumour growth (figure 6B). Flow cytometry analysis and IHC profiles suggested that the ratio of $CD8^+/CD4^+$ T cells and the production of IFN-γ, TNF-α and GZMB in $CD8^+$ T cells were increased both in the blood and tumours (figure 6C–F,H–M). We also observed fewer Treg cells in the combination group, which was associated with improved treatment efficacy (figure 6G). Meanwhile, we determined the content of tryptophan and kynurenine in mice plasma and found Kyn/Trp ratio decreased after combination treatment (figure 6J). Consistently, we also observed a lower IDO expression in tumour tissues after combination treatment (figure 6K,L). Collectively, these data revealed that GPs can sensitise the response to αPD-1 mAb in LLC-bearing mice.

Likewise, we examined whether combination treatment could modulate the gut microbiota in LLC tumour-bearing mice transplanted with gut microbiota from NRs. Excitingly, we found in combination group, the abundance of *Bacteroides*, especially *B. vulgatus* and *P. distasonis* were significantly increased when compared with αPD-1 mAb and Vehicle group, respectively (figure 6M,O, (online supplemental file 6A–C). No bacteria contamination during the GF cultivation condition was confirmed by time-course 16S rRNA sequencing (online supplemental file 7A–B). These results indicated that the combination treatment may reshape gut microbiota from NRs towards that of Rs to sensitise the response to αPD-1 mAb treatment.

DISCUSSION

PD-1 inhibitors are effective cancer immunotherapy in various types of cancer. However, the response rate needs to be largely improved. Accumulating numbers of clinical trials using combination therapies are currently in progress looking for enhanced sensitisation methods. GPs have also previously been reported to be an adjuvant drug for immunomodulation. Zhou *et al* demonstrated that GPs reinstate gut homeostasis, particularly by enhancing the growth of two major metabolic bacteria, *Lactobacillus* spp and *Bacteroides* spp., which may reverse overfatigue and acute cold stress phenotypes by enhancing host immune function.[36] *Bacteroides* spp. have a protective effect on gastrointestinal toxicity during CTLA-4 mAb treatment.[13] In the present study, we first observed that GPs combined with αPD-1 mAb could increase the SCFA-producing bacteria, *Muribaculum* to sensitise the antitumour effect of αPD-1 mAb in the LLC tumour-bearing mice. *Muribaculum* was the first genus found in *Muribaculaceae* which was also named *Bacteroidales S24-7*. *S24-7* was the predominant *Bacteroidetes* member in mice and was reported to be associated with better response to immunotherapy.[37] Whereas, in human subjects, the family *Bacteroidaceae* and the genus *Bacteroides* were the predominant *Bacteroidetes* members.[38] Besides, the difficulty to the culture of *S24-7* limited further research.[39] Our present study overscores the antitumour effect was attributable to the enhanced $CD8^+$ functional T cells and the downregulation of Treg cells by altering the gut microbiome.

Microbial metabolites intermediate the communication between microbiota and immune cells. SCFAs result from polysaccharide degradation by microbes. Whether SCFAs impact host physiology after treatment with αPD-1 mAb is still unclear. Nomura *et al* observed that the abundance of faecal SCFAs in solid cancer patients treated with nivolumab was higher in R than NR. These results suggest that increased SCFAs point to longer progression-free survival time.[40] In this study, we also observed that all the SCFAs including propionate, butyrate, isobutyrate, valerate, isovalerate and hexanoate, increased after treatment with αPD-1 mAb. In particular, valerate, which is commonly low in the plasma, was increased significantly after cotreatment with GPs and αPD-1 mAb compared with treatment with αPD-1 mAb alone. However, relatively little research has focused on valerate. We reason valerate may serve as HDAC inhibitor to delay tumour progression and upregulate immune response.[41 42] Further study will address whether valerate is potentially therapeutically useful for the αPD-1 mAb response and whether the microbiota is associated with this effect.

IDO activity has been proposed to be a possible mechanism of resistance to anti-PD-1 treatment, and several combination therapies have been launched into clinical trials.[43–45] Although the IDO-1 inhibitor, epacadostat (ECHO-301/KEYNOTE-252 trial) in combination with pembrolizumab, although in melanoma patients recently for many reasons,[46] IDO-1 is still a promising immune checkpoint which is associated with the attenuation of Treg cell activation.[47] The higher ratio of Kyn/Trp leads to the induction of Treg production and the suppression of T_{eff} cell production, as well as poor survival.[48 49] A previous study revealed that ginsenosides could decrease the concentration of kynurenine and the Kyn/Trp ratio in mouse plasma,[50] but whether GPs exhibit a similar effect is unknown. We *in vitro* fermented human faecal samples from healthy donors with GPs and found an increase in tryptophan and a reduction in kynurenine levels under both aerobic and anaerobic conditions. In addition, compared with αPD-1 mAb treatment alone, combination treatment led to a reduced Kyn/Trp ratio by reducing kynurenine but not tryptophan in mice. This result is consistent with the enhanced αPD-1 mAb response and increased survival time. Additionally, the peripheral Treg population decreased in response to the reduction in kynurenine. We also observed the decreased IDO activity in GF mice transferred microbiota from NRs. Collectively, GPs may improve the response to PD-1 inhibitor via decreasing IDO activity.

Previous studies show different groups got different microbes associated with the response to PD-1 inhibitor, which mainly concentrated on western people. Whether it is related to geographical differences remains to be seen. Jin *et al* enrolled 37 Chinese advanced NSCLC patients receiving nivolumab and patients using second-generation sequencing, found an enrichment of *Alistipes putredinis*, *Bifidobacterium longum* and *Prevotella copri* in responding patients, whereas *Ruminococcus_unclassified* was enriched in non-responding patients.[51] Here, we first examined the influence of the gut microbiota on the response of Asian patients with NSCLC to pembrolizumab using 16S PacBio SMRT sequencing. The results revealed enrichment of *B. vulgatus* and *P. distasonis* in Rs. *B. vulgatus* and *P. distasonis* are two species of commensal healthy bacteria.[52] *P. distasonis* has

been shown to enhance immune checkpoint inhibitor-mediated anticancer immunity by inducing the production of IFNγ$^+$CD8$^+$ T cells.[53 54] The genus *Bacteroides* enhance the antitumour effect and alleviate the gastrointestinal toxicity in melanoma patients treated with CTLA-4 blockade.[13]

Based on these studies, we investigated whether GPs in combination with αPD-1 mAb could reverse the response state. We transferred stool from 6 NRs to GF mice to study the effect of the gut microbiota on LLC-bearing mice. Excitingly, we found the abundance of *B. vulgatus* and *P. distasonis* were significantly increased after combination treatment compared with αPD-1 mAb or Vehicle group, respectively. This finding suggests that GPs sensitise the outcome of αPD-1 mAb therapy in recipient mice receiving faecal microbiota from NR donors by reshaping the gut microbiome from NRs towards that of Rs. Our GPs are commercially available as a dietary supplement, and we believe that our study can accelerate the clinical translation of GPs. Next, whether *B. vulgatus* and *P. distasonis* are the key orchestrators of the resistance to PD-1 inhibitors will be further investigated.

In summary, we revealed that GPs potentiate the antitumour effect of αPD-1 mAb by enhancing CD8$^+$ T cell function and reducing the suppressive effect of Tregs, which might be addressed by reshaping the gut microbiota and tryptophan metabolism. Additionally, we found that *P. distasonis* and *B. vulgatus* are over-represented among Chinese NSCLC Rs. Furthermore, the combination treatment increased the abundance of *B. vulgatus and P. distasonis* and reinstated the response to αPD-1 mAb in GF mice colonised with FMT from NR patients. Overall, our novel findings are summarised and illustrated in figure 7A,B. Our data indicate that GPs can be used as a dietary supplement for NSCLC patients to improve immunotherapy efficacy.

Author affiliations
[1]Dr Neher's Biophysics Laboratory for Innovative Drug Discovery/State Key laboratory of Quality Research in Chinese Medicine, Macau University of Science and Technology, Taipa, Macau, China
[2]Computational Virology Group, Center for Bacteria and Virus Resources and Application, Wuhan Institute of Virology Chinese Academy of Sciences, Wuhan, Hubei, China
[3]Precision Medicine Institute, Sun Yat-sen University First Affiliated Hospital, Guangzhou, Guangdong, China
[4]Department of Bacteriology, Capital Institute of Pediatrics, Chaoyang District, Beijing, China
[5]The Marine Biomedical Research Institute, Guangdong Medical University, Zhanjiang, Guangdong, China
[6]Joint Laboratory for Translational Cancer Research of Chinese Medicine of the Ministry of Education of the People's Republic of China, Guangzhou University of Chinese Medicine, Guangzhou, Guangdong, China
[7]Department of Oncology, Kiang Wu Hospital, Macau, Macau, China

Acknowledgements We would like to thank the Department of Pathology, University Hospital, Macau University of Science and Technology for the preparation of paraffin sections. We also appreciated Army Medical University for the supply of germ-free mice and Biocytogen for the supply of HuPD-1 mice.

Contributors EL-HL, YC, HW, JH and ZJ designed the study. JH, JY, ZJ, JL, XF, YZ, YX, HL, WW, YF, JL, AS, JC, JL, MY, LW, LL and RL performed the experiments. EL-HL, YC, DL, YW, WH, IK, HL, XY, YX, J-LW, QW and PY analysed the data. ZJ and XF carried out the FACS analysis. EL-HL, JH, YC, HW, ZJ and LL wrote the manuscript. All authors reviewed and approved the manuscript.

Funding This work was supported by Macao Science and Technology Development Fund (Project no: 0096/2018/A3, 001/2020/ALC), and the NSFC overseas and Hong Kong and Macao Scholars Cooperative Research Fund Project (Project no: 81828013).

Competing interests None declared.

Patient consent for publication Not required.

Ethics approval This study was conducted with the approval of the Kiang Wu Hospital, Macau. Ethics approval of animal studies were provided by Macau University of Science and Technology, the Third Army Medical University and the First Affiliated Hospital, Sun Yat-Sen University. All experiments were performed in compliance with institutional animal care guidelines and protocols approved by the committee.

Provenance and peer review Not commissioned; externally peer reviewed.

Data availability statement Data are available on reasonable request. All data relevant to the study are included in the article or uploaded as online supplemental information.

ORCID iDs
Jumin Huang http://orcid.org/0000-0002-7831-593X
Haizhou Liu http://orcid.org/0000-0002-4727-088X

REFERENCES

1 Bray F, Ferlay J, Soerjomataram I, *et al*. Global cancer statistics 2018: GLOBOCAN estimates of incidence and mortality worldwide for 36 cancers in 185 countries. *CA Cancer J Clin* 2018;68:394–424.
2 Rittmeyer A, Barlesi F, Waterkamp D, *et al*. Atezolizumab versus docetaxel in patients with previously treated non-small-cell lung cancer (oak): a phase 3, open-label, multicentre randomised controlled trial. *Lancet* 2017;389:255–65.
3 Garon EB, Rizvi NA, Hui R, *et al*. Pembrolizumab for the treatment of non-small-cell lung cancer. *N Engl J Med* 2015;372:2018–28.
4 Fehrenbacher L, Spira A, Ballinger M, *et al*. Atezolizumab versus docetaxel for patients with previously treated non-small-cell lung cancer (poplar): a multicentre, open-label, phase 2 randomised controlled trial. *Lancet* 2016;387:1837–46.
5 Vokes EE, Ready N, Felip E, *et al*. Nivolumab versus docetaxel in previously treated advanced non-small-cell lung cancer (CheckMate 017 and CheckMate 057): 3-year update and outcomes in patients with liver metastases. *Ann Oncol* 2018;29:959–65.
6 Borghaei H, Paz-Ares L, Horn L, *et al*. Nivolumab versus docetaxel in advanced Nonsquamous non-small-cell lung cancer. *N Engl J Med* 2015;373:1627–39.
7 Borcoman E, Kanjanapan Y, Champiat S, *et al*. Novel patterns of response under immunotherapy. *Ann Oncol* 2019;30:385–96.
8 Kim CG, Kim KH, Pyo K-H, *et al*. Hyperprogressive disease during PD-1/PD-L1 blockade in patients with non-small-cell lung cancer. *Ann Oncol* 2019;30:1104–13.
9 Gandhi L, Rodríguez-Abreu D, Gadgeel S, *et al*. Pembrolizumab plus chemotherapy in metastatic non-small-cell lung cancer. *N Engl J Med* 2018;378:2078–92.
10 Heinhuis KM, Ros W, Kok M, *et al*. Enhancing antitumor response by combining immune checkpoint inhibitors with chemotherapy in solid tumors. *Ann Oncol* 2019;30:219–35.
11 Chen DS, Mellman I. Elements of cancer immunity and the cancer-immune set point. *Nature* 2017;541:321–30.
12 Sivan A, Corrales L, Hubert N, *et al*. Commensal Bifidobacterium promotes antitumor immunity and facilitates anti-PD-L1 efficacy. *Science* 2015;350:1084–9.
13 Vétizou M, Pitt JM, Daillère R, *et al*. Anticancer immunotherapy by CTLA-4 blockade relies on the gut microbiota. *Science* 2015;350:1079–84.
14 Routy B, Le Chatelier E, Derosa L, *et al*. Gut microbiome influences efficacy of PD-1-based immunotherapy against epithelial tumors. *Science* 2018;359:91–7.
15 Gopalakrishnan V, Spencer CN, Nezi L, *et al*. Gut microbiome modulates response to anti-PD-1 immunotherapy in melanoma patients. *Science* 2018;359:97–103.
16 Sun Y-F, Zhang X, Wang X-Y, *et al*. [Effect of long-term intake of ginseng extracts on gut microbiota in rats]. *Zhongguo Zhong Yao Za Zhi* 2018;43:3927–32.
17 Quan L-H, Zhang C, Dong M, *et al*. Myristoleic acid produced by enterococci reduces obesity through brown adipose tissue activation. *Gut* 2020;69:1239–47.
18 Jia L, Zhao Y, Liang X-J. Current evaluation of the millennium phytomedicine- ginseng (II): collected chemical entities, modern pharmacology, and clinical applications emanated from traditional Chinese medicine. *Curr Med Chem* 2009;16:2924–42.
19 Yang S-H, Seo S-H, Kim S-W, *et al*. Effect of ginseng polysaccharide on the stability of lactic acid bacteria during freeze-drying process and storage. *Arch Pharm Res* 2006;29:735–40.
20 Sun Y. Structure and biological activities of the polysaccharides from the leaves, roots and fruits of Panax ginseng C.A. Meyer: an overview. *Carbohydr Polym* 2011;85:490–9.

21 Nishitsuji K, Xiao J, Nagatomo R, *et al*. Analysis of the gut microbiome and plasma short-chain fatty acid profiles in a spontaneous mouse model of metabolic syndrome. *Sci Rep* 2017;7:15876.
22 Qu C, Yuan Z-W, Yu X-T, *et al*. Patchouli alcohol ameliorates dextran sodium sulfate-induced experimental colitis and suppresses tryptophan catabolism. *Pharmacol Res* 2017;121:70–82.
23 Couter CJ, Surana NK. Isolation and flow cytometric characterization of murine small intestinal lymphocytes. *J Vis Exp* 2016;111. doi:10.3791/54114. [Epub ahead of print: 08 May 2016].
24 Graf J, Ledala N, Caimano MJ, *et al*. High-resolution differentiation of enteric bacteria in premature infant fecal Microbiomes using a novel rRNA amplicon. *mBio* 2021;12. doi:10.1128/mBio.03656-20. [Epub ahead of print: 16 Feb 2021].
25 Wolf AM, Wolf D, Steurer M, *et al*. Increase of regulatory T cells in the peripheral blood of cancer patients. *Clin Cancer Res* 2003;9:606–12.
26 Champiat S, Dercle L, Ammari S, *et al*. Hyperprogressive disease is a new pattern of progression in cancer patients treated by anti-PD-1/PD-L1. *Clin Cancer Res* 2017;23:1920–8.
27 Kamada T, Togashi Y, Tay C, *et al*. PD-1$^+$ regulatory T cells amplified by PD-1 blockade promote hyperprogression of cancer. *Proc Natl Acad Sci U S A* 2019;116:9999–10008.
28 Pelaseyed T, Bergström JH, Gustafsson JK, *et al*. The mucus and mucins of the goblet cells and enterocytes provide the first defense line of the gastrointestinal tract and interact with the immune system. *Immunol Rev* 2014;260:8–20.
29 Schewe M, Franken PF, Sacchetti A, *et al*. Secreted phospholipases A2 are intestinal stem cell niche factors with distinct roles in homeostasis, inflammation, and cancer. *Cell Stem Cell* 2016;19:38–51.
30 Ikpa PT, Sleddens HFBM, Steinbrecher KA, *et al*. Guanylin and uroguanylin are produced by mouse intestinal epithelial cells of columnar and secretory lineage. *Histochem Cell Biol* 2016;146:445–55.
31 Luo J, Han L, Liu L, *et al*. Catechin supplemented in a Fos diet induces weight loss by altering cecal microbiota and gene expression of colonic epithelial cells. *Food Funct* 2018;9:2962–9.
32 Ikpa PT, Meijsen KF, Nieuwenhuijze NDA, *et al*. Transcriptome analysis of the distal small intestine of CFTR null mice. *Genomics* 2020;112:1139–50.
33 Britton GJ, Contijoch EJ, Mogno I, *et al*. Microbiotas from humans with inflammatory bowel disease alter the balance of gut Th17 and RORγt$^+$ regulatory T cells and exacerbate colitis in mice. *Immunity* 2019;50:212–24.
34 Buck MD, O'Sullivan D, Pearce EL. T cell metabolism drives immunity. *J Exp Med* 2015;212:1345–60.
35 Rooks MG, Garrett WS. Gut microbiota, metabolites and host immunity. *Nat Rev Immunol* 2016;16:341–52.
36 Zhou S-S, Xu J, Zhu H, *et al*. Gut microbiota-involved mechanisms in enhancing systemic exposure of ginsenosides by coexisting polysaccharides in ginseng decoction. *Sci Rep* 2016;6:22474.
37 Uribe-Herranz M, Bittinger K, Rafail S, *et al*. Gut microbiota modulates adoptive cell therapy via CD8α dendritic cells and IL-12. *JCI Insight* 2018;3. doi:10.1172/jci.insight.94952. [Epub ahead of print: 22 Feb 2018].
38 Nagpal R, Wang S, Solberg Woods LC, *et al*. Comparative microbiome signatures and short-chain fatty acids in mouse, rat, non-human primate, and human feces. *Front Microbiol* 2018;9:2897.
39 Lagkouvardos I, Lesker TR, Hitch TCA, *et al*. Sequence and cultivation study of Muribaculaceae reveals novel species, host preference, and functional potential of this yet undescribed family. *Microbiome* 2019;7:28.
40 Nomura M, Nagatomo R, Inoue K, *et al*. Association of SCFA in gut microbiome and clinical response in solid cancer patients treated with andi-PD-1 antibody. *Ann Oncol* 2019;30:v509.
41 Luu M, Pautz S, Kohl V, *et al*. The short-chain fatty acid pentanoate suppresses autoimmunity by modulating the metabolic-epigenetic crosstalk in lymphocytes. *Nat Commun* 2019;10:760.
42 Laino AS, Betts BC, Veerapathran A, *et al*. Hdac6 selective inhibition of melanoma patient T-cells augments anti-tumor characteristics. *J Immunother Cancer* 2019;7:33.
43 Wang W, Huang L, Jin J-Y, *et al*. A validation study on IDO immune biomarkers for survival prediction in non-small cell lung cancer: radiation dose fractionation effect in early-stage disease. *Clin Cancer Res* 2020;26:282–9.
44 Jung KH, LoRusso P, Burris H, *et al*. Phase I study of the indoleamine 2,3-dioxygenase 1 (IDO1) inhibitor Navoximod (GDC-0919) administered with PD-L1 inhibitor (Atezolizumab) in advanced solid tumors. *Clin Cancer Res* 2019;25:3220–8.
45 Labadie BW, Bao R, Luke JJ. Reimagining IDO pathway inhibition in cancer immunotherapy via downstream focus on the Tryptophan-Kynurenine-Aryl hydrocarbon axis. *Clin Cancer Res* 2019;25:1462–71.
46 Sondak VK, Khushalani NI. Echoes of a failure: what lessons can we learn? *Lancet Oncol* 2019;20:1037–9.
47 Melaiu O, Lucarini V, Giovannoni R, *et al*. News on immune checkpoint inhibitors as immunotherapy strategies in adult and pediatric solid tumors. *Semin Cancer Biol* 2020. doi:10.1016/j.semcancer.2020.07.001. [Epub ahead of print: 10 Jul 2020].
48 Baban B, Chandler PR, Sharma MD, *et al*. Ido activates regulatory T cells and blocks their conversion into Th17-like T cells. *J Immunol* 2009;183:2475–83.
49 Li H, Bullock K, Gurjao C, *et al*. Metabolomic adaptations and correlates of survival to immune checkpoint blockade. *Nat Commun* 2019;10:4346.
50 Kang A, Hao H, Zheng X, *et al*. Peripheral anti-inflammatory effects explain the ginsenosides paradox between poor brain distribution and anti-depression efficacy. *J Neuroinflammation* 2011;8:100.
51 Jin Y, Dong H, Xia L, *et al*. The diversity of gut microbiome is associated with favorable responses to Anti-Programmed death 1 immunotherapy in Chinese patients with NSCLC. *J Thorac Oncol* 2019;14:1378–89.
52 Gu S, Zaidi S, Hassan MI, *et al*. Mutated CEACAMs disrupt transforming growth factor beta signaling and alter the intestinal microbiome to promote colorectal carcinogenesis. *Gastroenterology* 2020;158:238–52.
53 Tanoue T, Morita S, Plichta DR, *et al*. A defined commensal consortium elicits CD8 T cells and anti-cancer immunity. *Nature* 2019;565:600–5.
54 Gao J, Shi LZ, Zhao H, *et al*. Loss of IFN-γ pathway genes in tumor cells as a mechanism of resistance to anti-CTLA-4 therapy. *Cell* 2016;167:397–404.